Aerogels from polypyrrole/carbon nanotubes-based polymeric blends

René Salgado-Delgado[1), *)], Areli M. Salgado-Delgado[1)], Alfredo Olarte-Paredes[1)], Juan Carlos Ochoa-Jaimes[1)], Zully Vargas-Galarza[1)], Apolonio Vargas-Torres[2)], Teresa López-Lara[3)], Juan B. Hernández-Zaragoza[3)], Efraín Rubio-Rosas[4)], Victor M. Castaño[5)]

DOI: dx.doi.org/10.14314/polimery.2020.7.3

Abstract: Novel silica aerogels were produced from carbon nanotubes/carbon black/polypyrrole (NTC/CB/PPy) blends, and their structure characterized by FT-IR analysis. X-ray diffraction analysis confirms the presence of amorphous silica and a new reflection at $2\theta = 13°$, which had not been reported before. SEM micrographs of the aerogels reveal the connectivity of the micropores of the material, along with the different fillers (NTC/CB/PPy), which allow to increase the water absorption of the aerogels and to increase thermal stability. The mechanical and thermal properties of the resulting aerogels are significantly better than those of similar materials reported in the literature.

Keywords: aerogels, tetraethyl orthosilicate (TEOS), carbon nanotubes (NTC), polypyrrole (PPy), polymer gels.

Aerożele krzemionkowe na bazie polimerowych mieszanin polipirolu i nanorurek węglowych

Streszczenie: Otrzymano nowe aerożele krzemionkowe z wykorzystaniem mieszanin nanorurek węglowych, sadzy węglowej i polipirolu (NTC/CB/PPy). Strukturę wytworzonych aerożeli scharakteryzowano na podstawie widm FT-IR. Metodą dyfrakcji rentgenowskiej potwierdzono w nich obecność amorficznej krzemionki, stwierdzono też, wcześniej nieopisywane, odbicie przy $2\theta = 13°$. Mikrofotografie SEM aerożeli wykazały połączenia mikroporów krzemionki z cząstkami różnych napełniaczy (NTC/CB/PPy), pozwalające zwiększyć absorpcję wody przez aerożele i ich stabilność termiczną. Wykazano, że właściwości mechaniczne i termiczne powstałych aerożeli są znacznie lepsze niż właściwości podobnych materiałów opisanych w literaturze.

Słowa kluczowe: aerożele, ortokrzemian tetraetylu (TEOS), nanorurki węglowe (NTC), polipirol (PPy), żele polimerowe.

The synthesis of novel materials under controlled conditions allows to obtain molecular structures with specific characteristics such as elasticity, color, transparency, low chemical reactivity, electrical behavior, thermal and acoustic resistance, as well as resistance to fracture, among other properties [1, 2]. In 1930, Kistler proposed replacing the liquid phase of a hydrogel with a gas, which allowed him to produce the very first aerogel in 1931 [3]. Aerogels are nanostructured materials, obtained by extracting the liquid phase from a highly swollen hydrogel under certain conditions, in which there is a collapse of molecular network structure; this process is commonly carried out at temperature and pressure above the critical point of the solvent. The high porosity (up to 99%) and the nanotexture

[1)] Tecnológico Nacional de México (TecNM)/Instituto Tecnológico de Zacatepec (ITZ), Calzada Tecnológico No. 27, C.P. 62780, Zacatepec de Hidalgo, Morelos, México.

[2)] Instituto de Ciencias Agropecuarias, Universidad Autónoma del Estado de Hidalgo, Tulancingo, México.

[3)] Division de Estudios de Posgrado, Facultad de Ingeniería, Universidad Autónoma de Querétaro, Cerro de las Campanas S/N, Col. de las Campanas, 76010 Querétaro, México.

[4)] Benemérita Universidad Autónoma de Puebla, Centro Universitario de Vinculación y Transferencia de Tecnología, Prolongación de la 24 Sur y Av. San Claudio, Ciudad Universitaria, Col. San Manuel C.P. 72570 Puebla, México.

[5)] Centro de Física Aplicada y Tecnología Avanzada, Universidad Nacional Autónoma de México, Boulevard Juriquilla 3001, Querétaro 76230, México.

[*)] Author for correspondence: renesalgado@hotmail.com

of aerogels provide them very interesting properties, such as extremely low density (0.01–0.3 g/cm^3), high specific surface area (100–2000 m^2/g) and low thermal conductivity (<0.02 W/mK) [2, 4–6]. In general, the elaboration of aerogels comprises two main steps: the formation of a wet gel and the drying of the wet gel to form an aerogel. Different types of aerogels can be made using silica, alumina, chromium oxide, tin or carbon as a base. The vast majority of silica aerogels reported in recent years are made using silicone alkoxy precursors. The most commonly used are tetramethylorthosilane [TMOS: $Si(OCH_3)_4$] and tetraethylorthosilane [TEOS: $Si(OCH_2CH_3)_4$] [4, 5, 7–12]. Some of the industrial applications of aerogels include thermal insulation, acoustic insulation, catalyst support and aerospace applications [3, 13–17]. Good heat insulation is necessary in many fields, including the aerospace industry (aircrafts, spacecrafts), vehicles, civil construction, air conditioning systems and a great variety of industrial processes. Semiconductors have a lower electrical conductivity than metallic conductors but higher electrical conductivity than a good insulator. At very low temperatures, pure semiconductors behave as insulators. Subjected to high temperatures and mixed with impurities or in the presence of light, the conductivity of semiconductors can increase dramatically and reach levels close to those of metals. Given the great demand for aerogels that can be used for thermal insulation and electrical and mechanical conduction, it would be greatly useful to develop novel, more efficient materials for specific applications. Accordingly, the purpose of the present work was to produce novel aerogels made using a ternary mixture (carbon nanotubes/black smoke/polypyrrole) [18–22], to improve the thermal stability and the mechanical properties of aerogels reported in the literature or commercially-available.

EXPERIMENTAL PART

Materials

Tetraethyl orthosilicate (TEOS) CAS:78-10-4, $SiC_8H_{20}O_4$, 208.33 g/mol; hydrochloric acid (HCl) CAS: 7647-01-0; ethanol (CH_3CH_2OH) CAS: 64-17-5; ammonium hydroxide (NH_4OH), CAS: 1336-21-6; carbon nanotubes (NTC) Sigma-Aldrich CAS:308068-56-6; carbon black (CB), CB: Química Meyer, CAS: 1333-86-4; polypyrrole (PPy) Sigma-Aldrich CAS: 30604-81-0.

Ultrapure CO_2, Infra SA. de CV.

Preparation of aerogels

A mixture of TEOS/ethanol/water was prepared in a molar ratio of 1 : 9 : 6 in an ultrasonic bath with constant stirring. HCl 1 N was added until obtaining a pH = 2. The resulting mixture was placed in a sealed container and subjected to an ultrasonic bath at 60°C for 1 h. Afterwards, ammonium hydroxide was added in the same proportion as HCl, in addition, loads are added in different proportions and the stirring was kept for 24 h. The aerogels obtained were dried under supercritical conditions (1000 psi = 6.89 MPa) in a CO_2 atmosphere [23–25]. The same procedure was used for all the aerogels obtained in the present work. Loads are added in different proportions. The mixtures that contain a single charge such as TEOS-CB, TEOS-NTC and TEOS-PPy contain 99.4% of TEOS and 0.06% of each load. Binary mixtures such as TEOS-CB-NTC, TEOS-PPy-CB and TEOS-PPy-NTC contain 99.4% of TEOS and 0.03% of each charge. The TEOS-NTC-CB-PPy ternary mixture contains 0.02% of each load.

Methods of testing

Infrared spectroscopy

The samples of aerogel dust were analyzed by Fourier transform infrared (FTIR-ATR) analysis with a PerkinElmer model Spectrum Two, at room temperature (27°C). The samples were analyzed with 16 scans averaging 4 cm^{-1} resolution between 4000 cm^{-1} to 650 cm^{-1}. The FTIR-ATR analysis was used to characterize the presence of specific chemical groups of the materials.

Thermogravimetric analysis (TGA)

The thermogravimetric analysis (TGA) was performed (Netzsch, instrument STA449F3 Jupiter) by heating powdered samples from 25 to 800°C at 10°C/min in a nitrogen atmosphere.

X-ray diffraction (XRD)

This analysis was performed using an X-ray diffractometer (D8 Discovery, Bruker) at 40 kV and 40 mA with a radiation source of Cukα1, at a range 20 of 5–65° and 5–45°, using a step time of 43.2 s at room temperature.

Impedance spectroscopy (IES)

The samples of aerogel dust were analyzed by impedance spectroscopy (IES) with a Agilent model 4396B using a band frequency of 0 Hz to 7 MHz was applied. The above, to study the behavior of charge transfer and ion diffusion.

Scanning electron microscopy (SEM)

The samples were coated with a thin layer of gold by sputtering (Denton Vacuum, model Desk V) and their morphologies were observed under a scanning electron microscope JEOL model JSM-6010A that operated at voltage of 20 kV.

Variance analysis

The analysis was performed using an ANOVA table, with a level of significance of 0.05, establishing

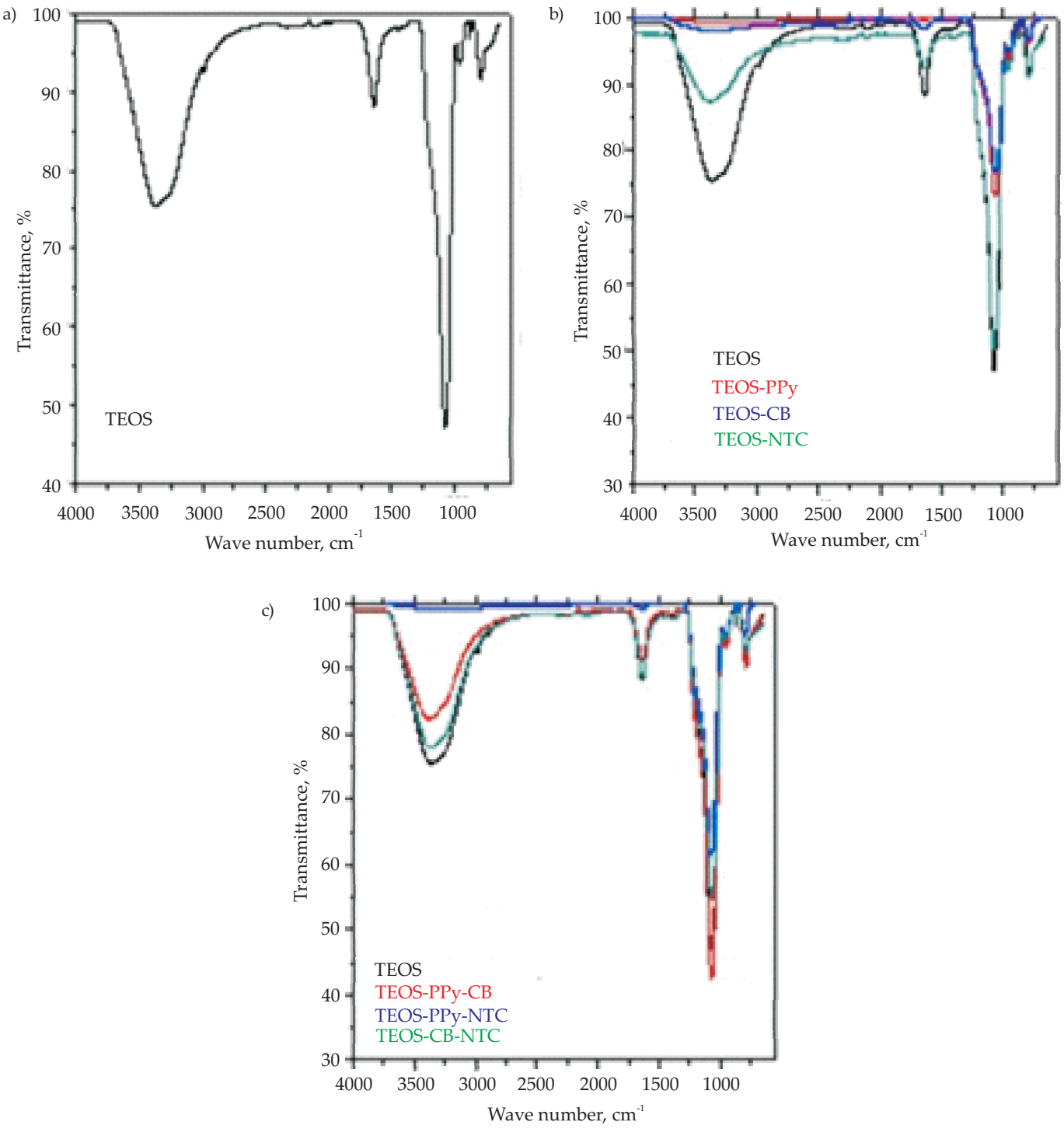

Fig. 1. FT-IR spectrum of: a) TEOS, b) TEOS, TEOS-NTC, TEOS-PPy, TEOS-CB, c) TEOS, TEOS-PPy-CB, TEOS-PPy-NTC and TEOS-CB-NTC

a Null Hypothesis Ho: TEOS = TEOS-CB = TEOS-NTC = TEOS-PPy = TEOS-CB-NTC = TEOS-PPy-CB = TEOS-PPy-NTC = TEOS-NTC-CB-PPy and an alternative hypothesis H1: The means of the treatments are different.

It was considered that

If F(calc) > F(Tab) then H1 is accepted and Ho is rejected.

If F(Tab) > F(calc) then Ho is accepted and H1 is rejected

RESULTS AND DISCUSSION

Infrared spectroscopy analysis (FT-IR)

The aerogels were characterized by FT-IR analysis. Figure 1 shows the FT-IR spectra of the aerogels, with the characteristic adsorption peaks. The peak at 1080 cm^{-1}

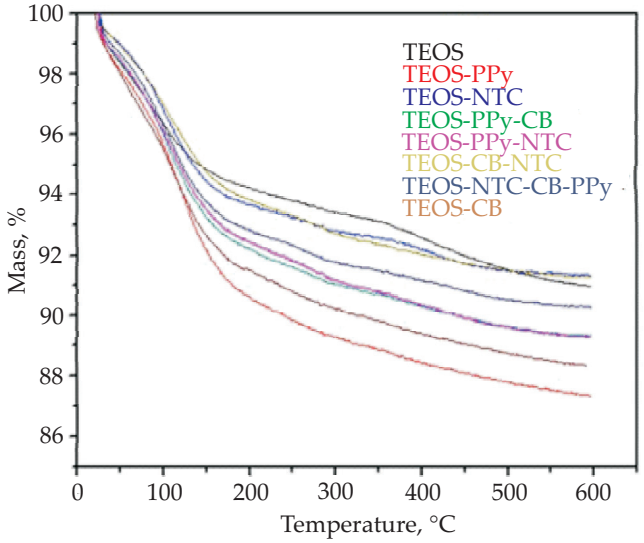

Fig. 2. Thermogravimetric analysis of silica aerogels (TEOS) and aerogels with the different loads (0.06% of the total load is used, it is distributed among the loads) used PPy, NTC, CB

T a b l e 1. Thermogravimetric analysis of the first stage of degradation and % mass loss

Aerogel: composite material	Temperature °C	Mass loss %
TEOS/CB	123.74	6.02
TEOS/PPy	122.02	6.00
TEOS/CB/NTC	111.52	3.59
TEOS/NTC	109.64	3.73
TEOS/NTC/CB/PPy	108.35	4.21
TEOS/PPy/NTC	107.18	4.36
TEOS/PPy/CB	105.54	4.40
TEOS	96.53	3.51

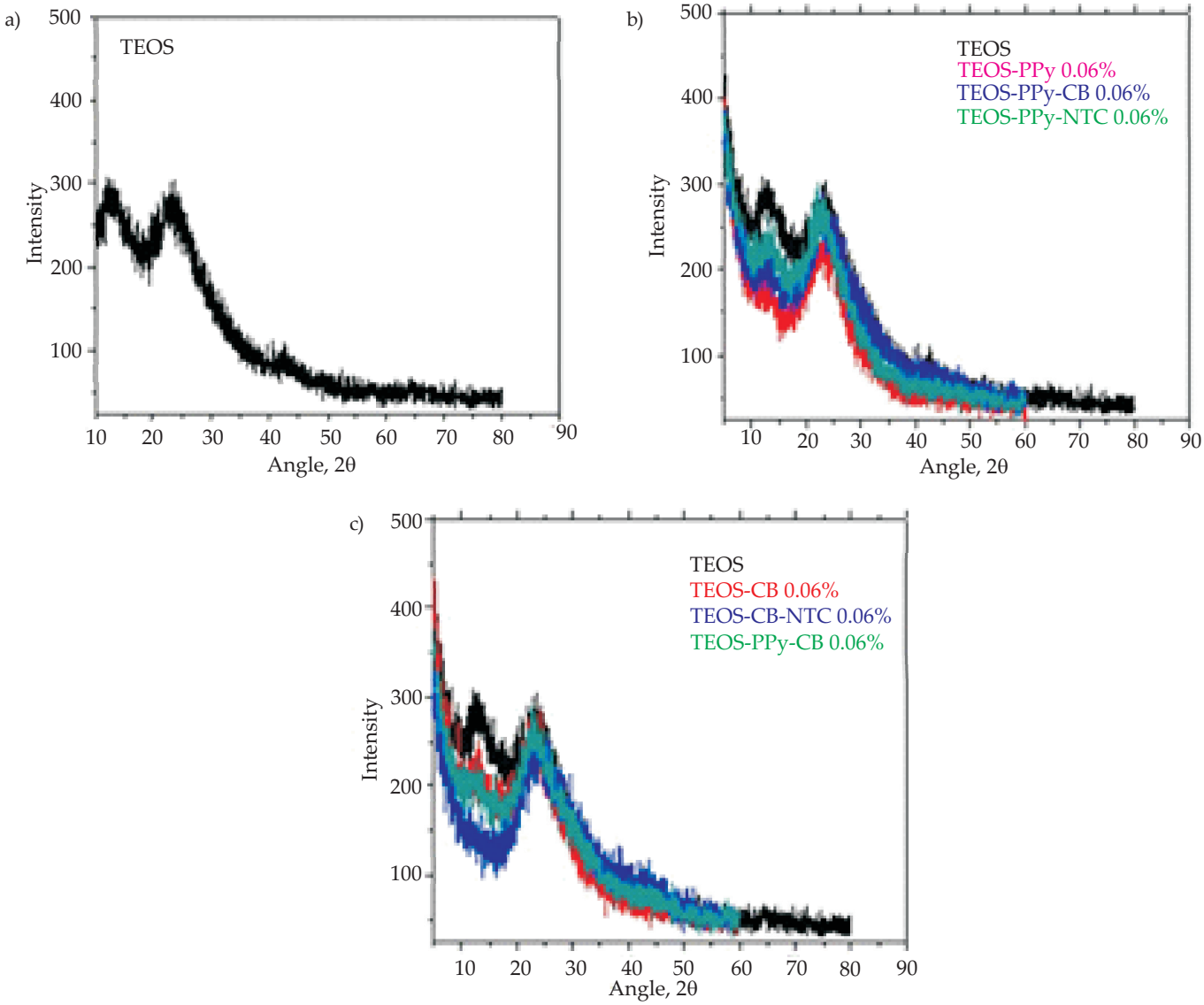

Fig. 3. X-ray diffraction of: a) TEOS, b), c) aerogels with the different loads (0.06% of the total load is used, it is distributed among the loads) used PPy, NTC, CB

corresponds to the stretching vibrational mode of the Si-O-Si of the TEOS structure (this signal has already been reported) [26, 27]. At 1600 cm^{-1} it is possible to observe a peak that corresponds to the stretching vibrational mode of the C=C present in polypyrrole and carbon nanotubes structures. The different fillers used caused the strength of the O-H stretch signal to decrease (3000–3500 cm^{-1}). This occurred due to the aliphatic structure of the fillers.

Thermal properties

In all cases, the results of thermogravimetric analysis show a mass loss at 105°C (Fig. 2), which is attributed mainly to the loss of water adsorbed from the material used to make the aerogels. The greatest loss of weight is observed in the range of 150°C to 500°C and is directly related to surface dehydroxylation in aerogels containing PPy, NTC or CB as a reinforcing material.

The above results are discussed in a previous work in which only PPy was used and that found that this load disappears at near 200°C [21]. Table 1 shows the TGA data of the samples. The results show that the loads used increased the thermal stability of the materials in the first stage of degradation, which corresponds to the release of the absorbed water. The thermal analysis of the obtained aerogels shows that the loads used in these materials reduced the percentage of waste.

X-ray diffraction

Figure 3 shows the X-ray diffractograms of the obtained aerogels, confirming the presence of a peak at approximately $2\theta = 23°$, as is typical for amorphous silica [18], and an angle of 26.6° (Fig. 3c), which corresponds to the amorphous part of the polypyrrole. However, our results also show a new peak at $2\theta = 13°$ that had not been reported before (Fig. 3c).

It is worth noting that when adding the loads this signal disappears, an indication of structural changes in the materials. It is possible to observe a diffraction angle of 26.6°, which corresponds to the amorphous band of the polypyrrole, and two diffraction angles at 24° and 44° that correspond to the carbon black, of which the first coincides with the amorphous structure of TEOS at 23°, and of polypyrrole at 26°. It should be noted that a signal of 44 is very small [20, 24].

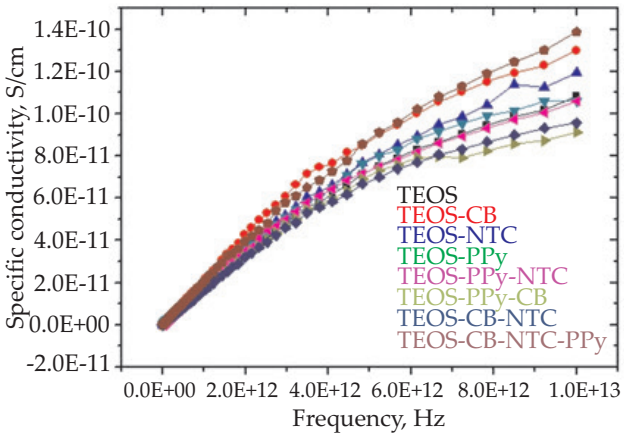

Fig. 4. Specific conductivity results of silica aerogels (TEOS) and aerogels with the different loads used PPy, NTC, CB

T a b l e 2. Electrical resistivity of silica aerogels (TEOS) and aerogels with the different loads used PPy, NTC, CB

Aerogel: composite material	Resistance, Ω
TEOS	7.12E+06
TEOS-CB	8.96E+06
TEOS-NTC	2.95E+06
TEOS-PPy	1.65E+06
TEOS-CB-NTC	1.63E+07
TEOS-PPy-CB	1.70E+07
TEOS-PPy-NTC	1.85E+07
TEOS-NTC-CB-PPy	4.34E+06

Impedance spectroscopy

Figure 4 shows the specific conductivity of the composite aerogels. The quaternary mixture TEOS-CB-NTC-PPy shows the highest value of electrical conductivity ($1.4 \cdot 10^{-10}$ S/cm), followed by the binary mixtures TEOS-CB, TEOS-NTC and TEOS-PPy. In general, the specific electrical conductivity of these binary mixtures is about $1.0 \cdot 10^{-10}$ to $1.2 \cdot 10^{-10}$ S/cm). The electrical conductivity of all the mixtures (binary, ternary and quaternary) is about $8 \cdot 10^{-11}$ to $1.4 \cdot 10^{-10}$ S/cm, with a frequency of $1 \cdot 10^{-13}$ Hz. There are reports of polyethylene with PPy with an electrical conductivity of $1.052 \cdot 10^{-10}$ S/cm (using concentrations of 5% of PPy) [28–31]. It is important to note that we can use a smaller load to achieve appropriate electrical conductivities.

T a b l e 3. Variance analysis of the results of the electrical conductivity of the composite aerogels

Origin of variations	Sum of squares	Degrees of freedom	Average of squares	F(calc)	Probability	Critical value for F(Tab)
Between groups	6.47E+14	7	9.24E+13	10691.72	3.06E-15	3.50
Within the groups	6.91E+10	8	8 645 527 621			
Total	6.47E+14	15				

H0: TEOS = TEOS-CB = TEOS-NTC = TEOS-PPy = TEOS-CB-NTC = TEOS-PPy-CB = TEOS-PPy-NTC = TEOS-NTC-CB-PPy
H1: The means of the treatments are different

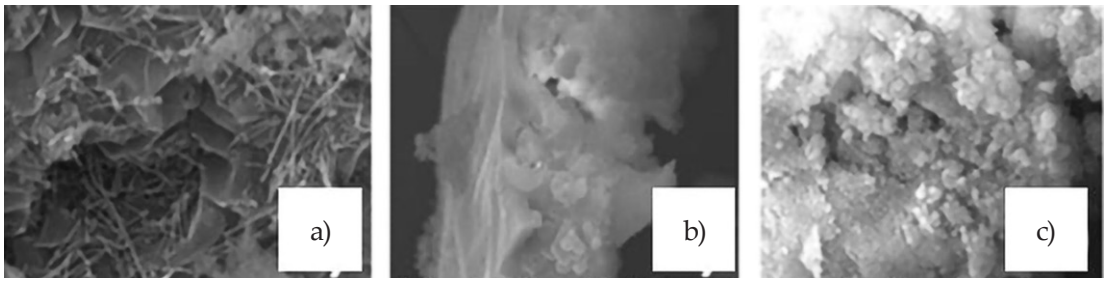

Fig. 5. SEM micrographs of composite aerogels: a) TEOS-NTC 8000×, b) TEOS-CB 2500×, c)TEOS-PPy 1500×

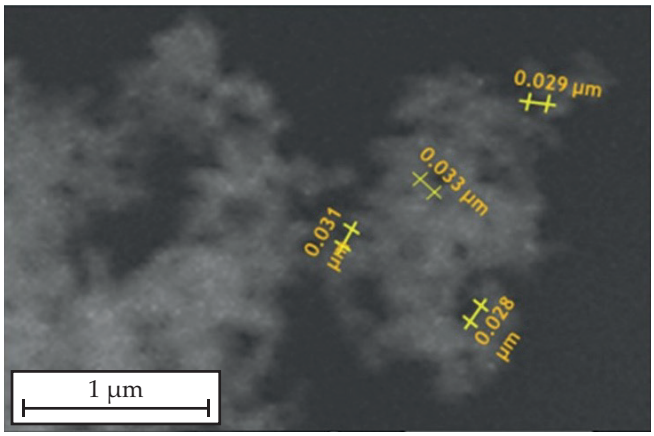

Fig. 6. SEM micrographs of composite aerogel TEOS-CB to 17000×

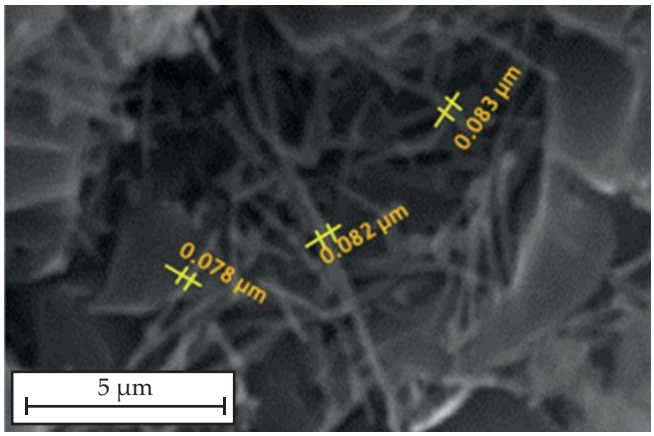

Fig. 7. SEM micrographs of composite aerogel TEOS-NTC to 5000×

Table 2 shows the results of electrical resistivity. It can be seen that the samples with low resistivity are the binary mixtures with TEOS-PPy and TEOS-NTC, as well as the quaternary mixture TEOS-CB-NTC-PPy. These samples were also those with greater conductivity.

Table 3 shows the results of a variance analysis of the response to electrical resistivity of the aerogels as a function of the loads.

The results show that F(calc) > F(Tab); therefore, H1 was accepted, demonstrating that the means of the treatments are different, which means that using different loads had a significant effect on the results.

Morphological characterization

The load distribution was analyzed using a JEOL scanning electron microscope (SEM) (JSM-6010A) in high vacuum mode (3500× and 20kV). Figure 5 shows the micrographs (SEM) of our aerogels. It is possible to see the porosity of the material, as well as the presence of some of the loads that were added to the aerogels, such as the NTC (Fig. 5a), CB (Fig. 5b) and PPy (Fig. 5c).

Figure 6 shows the micropores of the material. The aerogels have micropores of approximately 0.03 microns, corresponding to 33 nm. These micropores have been reported in works where they only obtain the TEOS aerogel which is corroborated in this work (SEM micrographs at 17000×), while Fig. 7 shows the diameter of the nanotubes, which is approximately 83 nanometers. In the literature, there are reports of aerogels made from TEOS that mention that the pores or internal spaces of the material measure from 50 to 100 nm, coinciding with the pores obtained by us [22].

CONCLUSIONS

Composite aerogels were obtained using the sol-gel process with different loads (NTC, CB, PPy), and subsequently dried under supercritical conditions. Composite aerogels were characterized by different techniques. FT-IR showed the different loads used and the functional groups characteristic of the network of aerogels made from TEOS. The addition of these loads gave certain hydrophilic properties to our aerogels, which absorbed more water and also had greater thermal stability during the first stage of degradation as a result of the hydrogen bonding links generated by water. The X-rays analysis showed that the presence of loads caused some structural changes in our material. Impedance spectroscopy showed that the addition of loads to our material contributed to produce an electrical conductivity response in the order of 10^{-10} (S/cm), as has already been reported in other works that used other loads. The statistical analysis showed that the loads had a significant effect on the electrical resistivity of the obtained aerogels, with a confidence level of 0.05 (5%).

The porosity of the aerogels was confirmed by SEM, with an average pore size of 0.03 micrometers, equivalent

to 33 nm. The results provide important information for future work related to the development of aerogels with useful electrical and thermal resistance properties.

REFERENCES

[1] Foladori G.: *Problemas de Desarrollo* **2016**, *47* (*186*), 59. https://doi.org/10.1016/j.rpd.2016.03.002

[2] Brostow W., Hagg Lobland H.E.: „Materiales: Introducción y Aplicaciones", John Wiley & Sons 2017.

[3] Kistler S.S.: *The Journal of Physical Chemistry* **1931**, *36* (*1*), 52. http://dx/doi.org/10.1021/j150331a003

[4] Anderson A.M., Wattley C.W., Carroll M.K.: *Journal of Non-Crystalline Solids* **2009**, *355* (*2*), 101.

[5] Sarawade P.B, Kim J.K., Kim H.K., Kim H.T.: *Applied Surface Science* **2007**, *254*, (2), 574. https://doi.org/10.1016/j.apsusc.2007.06.063

[6] Hrubesh L.W.: *Journal of Non-Crystalline Solids* **1998**, *225*, 335. https://doi.org/10.1016/S0022-3093(98)00135-5

[7] Tamon H., Kitamura T., Okazaki M.: *Journal of Colloid Interface Science* **1998**, *197,* 353. https://doi.org/10.1006/jcis.1997.5269

[8] Gleiter H.: *Nanostructured Materials* **1995**, *6*, 3. https://doi.org/10.1016/0965-9773(95)00025-9

[9] Ślosarczyk A.: *Journal of Sol-Gel Science and Technology* **2017**, *84*, 16. http://dx.doi.org/10.1007/s10971-017-4470-4

[10] Linhares T., Pessoa de Amorim M.T., Durães L.: *Journal of Materials Chemistry A* **2019**, *7*, 22768. https://doi.org/10.1039/C9TA04811A

[11] Li X., Feng J., Yin J. *et al*.: *Nanomaterials* **2019**, *9*, 40. http://dx.doi.org/10.3390/nano9010040

[12] Arce H., Montero M., Sáenz y A., Castaño V.M.: *Polyhedron* **2004**, *23*,1897.

[13] Cuce E., Cuce P.M., Wood C.J., Riffat S.B.: *Renewable and Sustainable Energy Reviews* **2014**, *34*, 273. https://doi.org/10.1016/j.rser. 2014.03.017

[14] Memioğlu F., Bayrakçeken A., Öznülüer T., Ak M.: *International Journal of Hydrogen Energy* **2012**, *37* (*21*), 16673. http://dx.doi.org/10.1016/j.ijhydene.2012.02.086

[15] Macías C., Haro M., Parra J.B. *et al*.: *Carbon* **2013**, *63*, 487. https://doi.org/10.1016/j.carbon.2013.07.024

[16] Li Z., Cheng X., He S. *et al*.: *Journal of Sol-Gel Science and Technology* **2015**, *76* (*1*), 138. http://dx.doi.org/10.1007/s10971-015-3760-y

[17] Li Z., Gong L., Cheng X. *et al*.: *Materials & Design* **2016**, *99*, 349. https://doi.org/10.1016/j.matdes.2016.03.063

[18] Tadjarodi A., Haghverdi M., Mohammadi V.: *Materials Research Bulletin* **2012**, *47* (*9*), 2584. https://doi.org/10.1016/j.materresbull.2012.04.143

[19] Noparvar-Qarebagh A., Roghani-Mamaqani H., Salami-Kalajahi M.: *Microporous and Mesoporous Materials* **2016**, *224*, 58 https://doi.org/10.1016/j.micromeso.2015.10.012

[20] Rasines G., Lavela P., Macías C. *et al*.: *Journal of Electroanalytical Chemistry* **2015**, *741*, 42. https://doi.org/10.1016/j.jelechem.2015.01.016

[21] Cheng Q., Pavlinek V., Li C. *et al*.: *Materials Chemistry and Physics* **2006**, *98*, 504. https://doi.org/10.1016/j.matchemphys.2005.09.074

[22] Jennings A.R., McCollum J., Wilkins A.J. *et al*.: *RSC Advances* **2017**, *7*, 21962. http://dx.doi.org/10.1039/C7RA02016C

[23] Guangwu L., Xingyuan N., Yangang L.: 10th IEEE International Conference on Nano/Micro Engineered and Molecular Systems, 7–11 April 2015, Xi'an, China. http://dx.doi.org/10.1109/NEMS.2015.7147399

[24] Zhou S., Wang M., Chen X., Xu F.: *ACS Sustainable Chemistry* **2015**, *3*, (*12*), 3346. http://dx.doi.org/10.1021/acssuschemeng.5b01020

[25] Yang Q., Wang L., Xiang W. *et al*.: *Polymer* **2007**, *48*, (*12*), 3444. https://doi.org/10.1016/j.polymer.2007.02.064

[26] Muller D., Pinheiro G.K., Bendo T. *et al*.: *Journal of Nanomaterials* **2015**, ID 658476. http://dx.doi.org/10.1155/2015/658476

[27] Al-Oweini R., El-Rassy H.: *Journal of Molecular Structure* **2009**, *919* (*1–3*), 140. https://doi.org/10.1016/j.molstruc.2008.08.025

[28] Ying S., Zheng W., Li B. *et al*.: *Synthetic Metals* **2016**, *218*, 50. http://dx.doi.org/10.1016/j.synthmet.2016.05.002

[29] Nahar L., Arachchige I.U.: *JSM Nanotechnology and Nanomedicine* **2013**, *1* (*1*), 1004.

[30] Tang W., Santare M.H., Advani S.G.: *Carbon* **2003**, *41* (*14*), 2779. http://dx.doi.org/10.1016/S0008-6223(03)00387-7

[31] Salgado-Delgado R., Olarte-Paredes A., Salgado-Delgado A.M. *et al*.: *Acta Universitaria* **2016**, *26* (*2*), 55. http://dx.doi.org/10.15174/au.2016.980

Received 14 I 2020.